

An efficient algorithm to estimate the potential barrier height from noise-induced escape time data

Tamás Bócai^{1,2}

¹Centre for the Mathematics of Planet Earth, University of Reading, UK

²Department of Mathematics and Statistics, University of Reading, UK

August 22, 2018

It is a common phenomenon in nature and technology that a system under perturbations exits a regime of its usual dynamics [1, 2, 3, 4, 5, 6]. Often it is possible to define a potential function whereby a potential well can be associated with a usual or persistent dynamics, and a saddle of the potential adjacent to the potential well is a feature through which the exit takes place [7]. The potential difference between the bottom of the potential well and the saddle is often termed a potential barrier. The expected exit time then depends on the height of this potential barrier and the (small) noise strength. Therefore, knowing the potential barrier height is often of strong interest, because then one can predict – for a given or applied noise strength – the expected escape time.

We develop an algorithm to determine the potential barrier height experimentally, provided that we have control over the noise strength. We are concerned with the situation when the experiment requires large resources of time or computational power, and wish to find a protocol that provides the best estimate in a given amount of time. We encountered such a situation when wanted to determine expected transition times to a cold climate for a noisy version of the climate model presented in [8].

We consider the rather generic situation when the dynamics is governed by the following Langevin stochastic differential equation (SDE):

$$\dot{\mathbf{x}} = \mathbf{F}(\mathbf{x}) + \sigma \mathbf{D} \boldsymbol{\xi}(t), \quad (1)$$

$\mathbf{x}, \mathbf{F}, \boldsymbol{\xi} \in \mathbb{R}^n$, and the diffusion matrix $\mathbf{D} \in \mathbb{R}^{n \times n}$ is independent of \mathbf{x} , i.e., the white noise $\boldsymbol{\xi}$ is additive. The vector field $\mathbf{F}(\mathbf{x})$ is such that it realises the coexistence of multiple attractors (including the possibility of an attractor at infinity) and at least one nonattracting invariant set, often called a saddle set. The saddle set is embedded in the boundary of some basins of attraction. Based on a well-established theory due to Freidlin and Wentzell [9] the steady state probability distribution in the weak-noise limit, $\sigma \ll 1$, can be written as

$$W(\mathbf{x}) \sim Z(\mathbf{x}) \exp(-2\Phi(\mathbf{x})/\sigma^2), \quad (2)$$

in which $\Phi(\mathbf{x})$ is called the nonequilibrium- or quasi-potential. In gradient systems where $\mathbf{F}(\mathbf{x}) = -\nabla V(\mathbf{x})$ we have that $\Phi(\mathbf{x}) = V(\mathbf{x})$, provided that $\mathbf{D} = \mathbf{I}$. If \mathbf{D} does depend on \mathbf{x} , then $W(\mathbf{x})$ might not satisfy a large deviation law $\lim_{\sigma \rightarrow 0} \sigma^2 \ln W(\mathbf{x}) = -2\Phi(\mathbf{x})$. See e.g. [10] for an example of multiplicative noise where $\lim_{\sigma \rightarrow 0} \sigma^2 \ln W(\mathbf{x} = x)$ does not exist for some parameter setting and $W(x)$ has a fat tail.

The probability that a perturbed trajectory does not escape the basin of attraction over a time span of t_t decays exponentially:

$$P(t_t) \sim \frac{1}{\tau} \exp(-t_t/\tau). \quad (3)$$

The approximation is in fact quite good already for times $t_t \approx \mathbb{E}[t_t] = \tau$ or even smaller. The reciprocal of the expectation value τ can be written as an integral of the probability current through the basin boundary, whose leading component as $\sigma \rightarrow 0$ comes from a point \mathbf{x}_e where $\Phi(\mathbf{x})$ is minimal on the boundary. The proportionality of the probability current to $W(\mathbf{x})$ leads [11, 12] to:

$$\tau \propto \exp(2\Delta\Phi/\sigma^2), \quad (4)$$

where

$$\Delta\Phi = \Phi(\mathbf{x}_e) - \Phi(A) \quad (5)$$

is what we call the potential barrier height. Both the saddle and the attractor can be chaotic, in which cases $\Phi(\mathbf{x}_e)$ and $\Phi(A)$ have been shown [13, 14] to be constant over the saddle [13] and attractor [14], respectively.

Considering (4), the expected transition times increase “explosively” as the noise strength σ decreases. From the point of view of estimating $\Delta\Phi$, there seems to be a trade-off between an increasing accuracy of the estimation and an increasing demand of resources as σ decreases. However, if we fix the amount of resources that we are willing to commit, then an increasing of accuracy is not guaranteed any more, because we can register fewer transitions as σ decreases. On the other hand, increasing σ beyond a point might not improve accuracy

either for the following reason. We assume that for some σ_0 we can estimate $\tau = \tau_0$ arbitrarily accurately because a large number of transitions can be achieved inexpensively. We also assume that in this ‘‘anchor point’’ (4) applies accurately:

$$\tau \approx \tau_0 \exp(2\Delta\Phi(\sigma^{-2} - \sigma_0^{-2})), \quad \sigma < \sigma_0. \quad (6)$$

Then, we can identify the accuracy of estimation by

$$\delta\Delta\Phi = \frac{\sqrt{\text{Var}[\ln \bar{t}_t]}}{y}, \quad (7)$$

where we introduced $y = \sigma^{-2} - \sigma_0^{-2}$, and $\bar{t}_t = \frac{1}{N} \sum_{i=1}^N t_i$ is our finite- N estimate of τ for a fixed σ . Clearly, as $\sigma \rightarrow \sigma_0$ the inaccuracy explodes. That is, in the described setting of estimation (which is not the most generic one) there should exist an optimal value of σ .

The sum of the exponentially distributed random variables, $N\bar{t}_t$, does in fact follow an Erlang distribution [15], and so:

$$P(\bar{t}_t) \sim \frac{1}{\tau^N} \frac{(N\bar{t}_t)^{N-1}}{(N-1)!} \exp(-N\bar{t}_t/\tau)N. \quad (8)$$

Note that since $E[\bar{t}_t] = E[t_t] = \tau$, our estimator \bar{t}_t is unbiased. Furthermore, $\text{Var}[\bar{t}_t] = \text{Var}[t_t]/N = \tau^2/N$ in accordance with the Central Limit Theorem. From (8) it follows that

$$\text{Var}[\ln \bar{t}_t] = \Psi^{(1)}(N), \quad (9)$$

where $\Psi^{(1)}(N)$ is the first derivative of the digamma function [16]. We can make the interesting observation that $\text{Var}[\ln \bar{t}_t]$ does not depend on τ , only on N . Next, we make use of the approximation [16]

$$\Psi^{(1)}(N) \sim 1/N \quad (10)$$

writing

$$\delta\Delta\Phi \sim \sqrt{\frac{\tau_0}{T}} \frac{\exp(\Delta\Phi y)}{y}, \quad (11)$$

where we, first, assumed a certain fixed commitment of resources, which can be expressed simply by $T = N\tau$, and, second, made use of (6). We look for a $\sigma = \sigma^*$ or $y = y^*$ that minimizes $\delta\Delta\Phi$, for which we need to solve $d\delta\Delta\Phi/dy = 0$, yielding our main result:

$$y^* = \Delta\Phi^{-1}. \quad (12)$$

We can make the interesting observation that it is independent of τ_0 and T , which we comment on shortly. y^* depends only on $\Delta\Phi$ (in a very simple way), the unknown that we wanted to determine in the first place, and so the result can seem irrelevant to practice for the first sight. However, one can simply start out with an

initial guess value, $\hat{\Delta\Phi}_0$, and iteratively update the estimate as $\hat{\Delta\Phi}_i$ by performing a maximum likelihood estimation (MLE) [17] each time a new value of $t_{t,i}$ is acquired. This way, for the acquisition of $t_{t,i+1}$, one continues the experiment with an updated noise strength $y_{i+1}^* = \hat{\Delta\Phi}_i^{-1}$, $i = 1, \dots, N$, according to (12). The MLE of $\Delta\Phi$ is based on the probability distribution (3) jointly with (6). This is an analogous procedure to non-stationary extreme value statistics when one or more parameters of the extreme value distribution (EVD) is a function of a covariate that could depend on time. In our case τ and σ correspond to the EVD parameter and covariate, respectively. We note that as σ^* does not depend on T , at any time into the experiment (for large enough N , though, such that (10) is a good approximation) our estimate of $\Delta\Phi$ is done most efficiently, and so we can revise our commitment, either stopping the experiment early or extending it. Next we demonstrate the use of our algorithm on two examples; in a single- as well as a multi-dimensional system.

Example 1: Overdamped particle in a symmetrical 1D double-well potential. It is governed by the following SDE:

$$dx = -V'dt + \sigma dW. \quad (13)$$

We specify our example as: $V = x^4/4 - x^2$. The two minima are at $x_{\pm} = \pm\sqrt{2}$, and the local maximum in between is at $x_0 = 0$. These are fixed points of the deterministic case ($\sigma = 0$). A numerical solution of the SDE (13) is obtained by using an Euler-Maruyama integrator [18] with a time step size of $h = 0.02$. Examples are shown in Fig. 1, indicating the regime behaviour with irregular transitions between the two regimes. The time series clearly evidence bimodal marginal distributions – corresponding to the two regimes – whose maxima, and the local minimum in between (not shown), are exactly at $x_{\pm} = \pm\sqrt{2}$ and $x_0 = 0$, respectively. With substituting these in to (5) we obtain that $\Delta V = \Delta\Phi = 1$. This shows up as the slope of the curve in Fig. 2. The green coloring indicates that (4) is satisfied well even with so strong noise that the time spent in a regime is not so clear cut any more, as seen in Fig. 1 (a). The result of applying our algorithm is shown in Fig. 3, indicating that it serves its purpose, and that the convergence is rather fast. Finally, Fig. 4 verifies the corner stone of the algorithm (12), showing the sample standard deviation of a number of estimates. Results with the algorithm and different fixed sample values of σ are shown in one diagram, indicating that the accuracy of estimate by our algorithm is just about the best accuracy achievable by the same amount of computation using the optimal fixed σ . Note that we chose $N = 30$ for our algorithm, resulting in some computational time T , and then we realised $N = \lceil T/\tau(\sigma) \rceil$ transitions using the different fixed σ 's.

Example 2: The Ghil-Sellers energy balance climate model (GSEBM). One of the most striking facts about

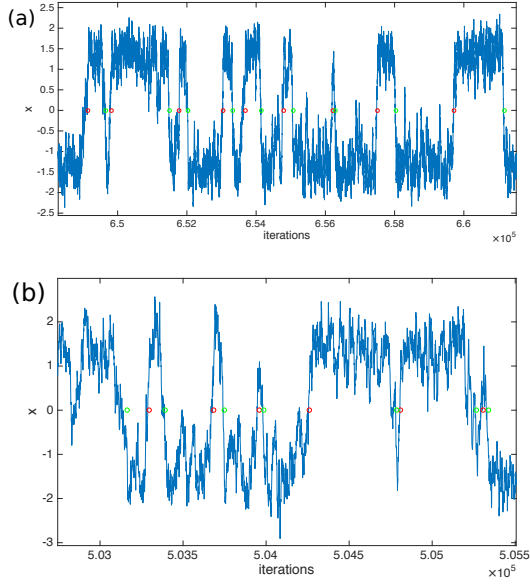


Figure 1: Numerical solution of (13). (a) $\sigma = 1.0$, (b) $\sigma = 1.55$. Red and green circle markers indicate transition times defined as a first crossing to the bottom of the upper (lower) potential well since a crossing to the lower (upper) well.

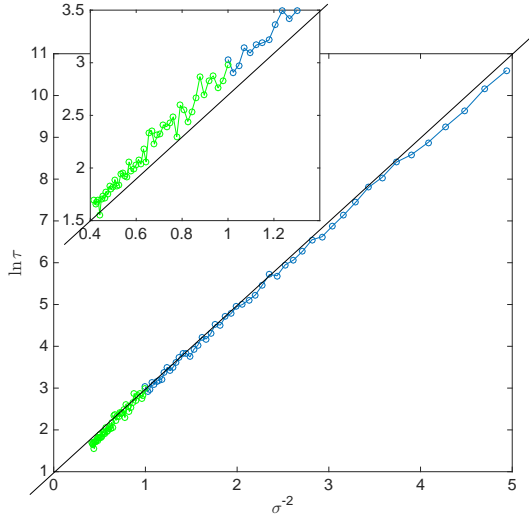


Figure 2: Demonstration of the validity of (4) in (13). A straight line of slope $\Delta V = 1$ is included in the diagram for reference. To estimate τ we averaged $N = 200$ transition times each sample values of σ corresponding to a circle marker.

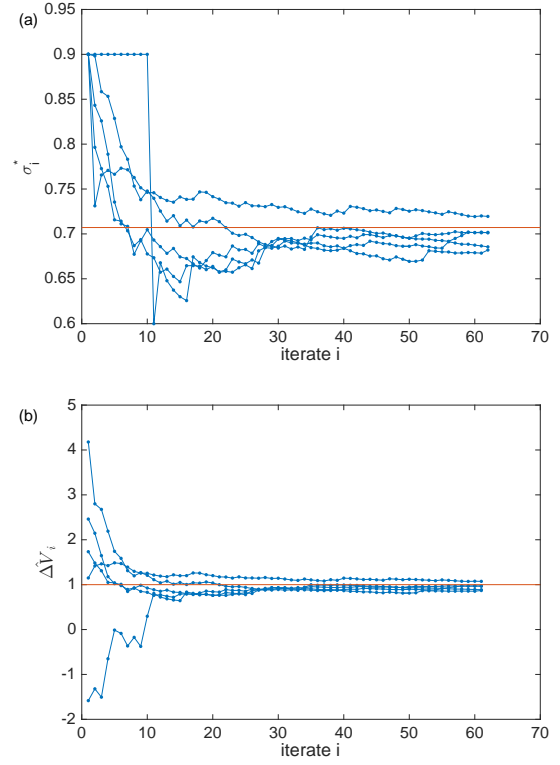


Figure 3: Proof of concept, I: convergence of estimates $\Delta \hat{\Phi}_i$. The anchor τ_0 was established with $\sigma_0 = 1$ using $N = N_0 = 400$. Five different realizations of the experiment are shown. The initial value for each is $\sigma_0^* = 0.9 < \sigma_0$. A “safeguarding” of the procedure is facilitated by overriding (12) such that $\sigma_{i+1}^* = \sigma_0$ if $\Delta \hat{\Phi}_i < 0$ and $\sigma_i^* = \sigma_{min}^* = 0.6$ when (12) dictates smaller.

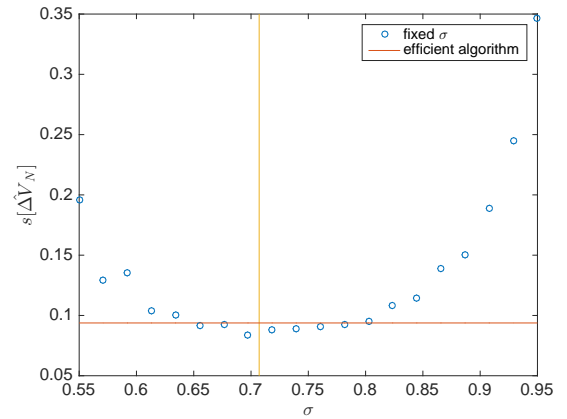


Figure 4: Proof of concept, II: sample standard deviation of 200 estimates $\Delta \hat{V}_N$. For the efficient algorithm we chose $N = 30$, which implies (see the main text) the different N 's for the different fixed sample values of σ . The vertical line marks the prediction of (12).

Earth's climate is its bistability: beside the relatively warm climate that we live in, under the present astronomical conditions a very cold climate featuring a fully glaciated so-called snowball Earth is also possible, and this state might have been experienced a number of times by Earth in the past few hundred million years [19]. Different hypotheses of transitioning from the warm to the cold climate and the other way round involve external forcings, but in principle it is possible that the climate system is transitive, at least in the warm-to-cold direction. This transitivity can be modeled by noise-induced transition, where the noise models some unresolved internal, say, atmospheric and/or oceanic dynamics. Without a requirement for physical realism, we consider additive noise perturbations of the Ghil-Sellers model [20] written for the long time average surface air temperature $T(\phi, t)$ as a function of latitude $\phi \in [-\pi/2, \pi/2]$ or $x = 2\phi/\pi \in [-1, 1]$. The deterministic GSEBM stands in the form of a diffusive heat equation:

$$C(x)\partial_t T(t, x) = \mu Q(x)(1 - \alpha(x, T)) - O(T) + M(x)\partial_x[(D_1(x) + D_2(x)g(T))\partial_x T]. \quad (14)$$

See [20, 21] for the concrete form of the equation and the meaning of its terms, and [22] for a numerical implementation. Unlike [22] that uses Matlab's `pdepe`, here we simulate the noise-perturbed GSEBM by Matlab's `simulate`. For this we discretize the eq. with respect to T by the method of lines, converting the PDE in to an ODE, i.e., eq. (1). The particular difference schemes that we apply using a regular grid are:

$$\begin{aligned} \partial_x[D_1(x)\partial_x T] &\approx [(T_{j+1} - T_j)D_{1,j+1/2} - \\ &\quad (T_j - T_{j-1})D_{1,j-1/2}]/\Delta x^2, \\ \partial_x[D_2(x)g(T)\partial_x T] &= \partial_x[D_2(x)\partial_x G] \approx \\ &\quad [(G(T_{j+1}) - G(T_j))D_{2,j+1/2} - \\ &\quad (G(T_j) - G(T_{j-1}))D_{2,j-1/2}]/\Delta x^2, \end{aligned} \quad (15)$$

$j = 1, \dots, J$, where $T_j \approx T(x_j)$, $x_j = (j-1/2)\Delta x - 1$, $\Delta x = 2/J$, and $D_{1,j\pm 1/2} = D_1(x_{j\pm 1/2})$, $x_{j\pm 1/2} = x_j \pm \Delta x/2$ (see p. 1046 of [23] regarding the x -dependent diffusivity). The boundary conditions are eliminated by the method of reflection, setting $T_0 = T_J$ and $T_{J+1} = T_1$. Such a grid deals effectively with the singularity of $M(x)$ at the poles, but the resulting ODE can be somewhat stiff. Fig. 5 shows that our algorithm works also in a multi-dimensional setting.

Acknowledgments

I would like to thank Ying Tang for his extremely helpful support for using their code [3], and Tamás Tél for providing valuable feedback on a draft of the

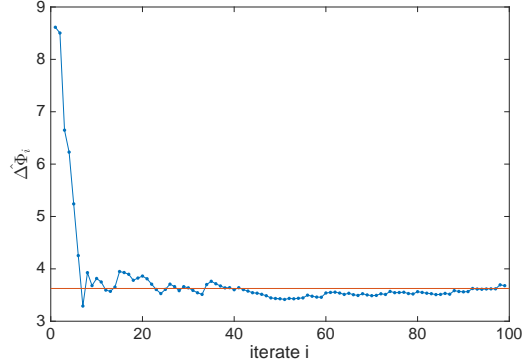


Figure 5: Same as Fig. 3 (b) but for the discretized GSEBM, $J = 10$, and $\sigma_0 = 1.7$, $N_0 = 400$, $\sigma_0^* = 1.5$, $\sigma_{min}^* = 1.0$. We considered only warm-to-cold transitions given the present day solar strength $\mu = 1$. The red line marks the potential difference $\Delta\Phi$ between the warm climate and the saddle. Note that here we measure time in 10^6 seconds [Ms], as a change to [22, 21]. An expression for the potential functional $\Phi(T)$ of the PDE was given in [20]. However, we calculate $\Delta\Phi$ for the discretized system by an action-minimizing procedure [3], using the computer code as a supplementary material to that paper. Time-discretization of the instanton was realised by 100 points over a span of 2000 [Ms]. Note that for the feasibility of the minimization it is crucial to provide symbolically the gradient of the action with respect to the displacement of the discrete sample points of the instanton. To be able to achieve this using the code of [3] the method of lines has to result in an explicit expression for \dot{T}_j . This could not be achieved by the sophisticated method implemented in Matlab's `pdepe`, which is why we developed the discretization scheme (15).

manuscript. I would like to acknowledge Valerio Lucarini for the many inspiring exchanges on the topic of critical transitions. This work received funding from the EU Blue-Action project (under grant No. 727852).

References

- [1] Christian Kuehn, Erik A. Martens, and Daniel M. Romero. Critical transitions in social network activity. *Journal of Complex Networks*, 2(2):141–152, 2014.
- [2] Vasilis Dakos and Jordi Bascompte. Critical slowing down as early warning for the onset of collapse in mutualistic communities. *Proceedings of the National Academy of Sciences*, 111(49):17546–17551, 2014.
- [3] Ying Tang, Ruoshi Yuan, Gaowei Wang, Xiaomei Zhu, and Ping Ao. Potential landscape of high dimensional nonlinear stochastic dynamics with large noise. *Scientific Reports*, 7(1):15762, 2017.
- [4] Davide Faranda, Valerio Lucarini, Paul Manneville, and Jeroen Wouters. On using extreme values to detect global stability thresholds in multistable systems: The case of transitional plane couette flow. *Chaos, Solitons & Fractals*, 64:26–35, 2014.
- [5] Dénes Takács, Gábor Stépán, and S. John Hogan. Isolated large amplitude periodic motions of towed rigid wheels. *Nonlinear Dynamics*, 52(1):27–34, Apr 2008.
- [6] Ulrike Feudel, Alexander N. Pisarchik, and Kenneth Showalter. Multistability and tipping: From mathematics and physics to climate and brainminireview and preface to the focus issue. *Chaos: An Interdisciplinary Journal of Nonlinear Science*, 28(3):033501, 2018.
- [7] Hannes Risken. *The Fokker-Planck equation*. Springer, 1996.
- [8] Valerio Lucarini and Tamás Bódai. Edge states in the climate system: exploring global instabilities and critical transitions. *Nonlinearity*, 30(7):R32, 2017.
- [9] M. I. Freidlin and A.D. Wentzell. *Random Perturbations of Dynamical Systems*. Springer, New York, 1984.
- [10] Tamás Bódai and Christian Franzke. Predictability of fat-tailed extremes. *Phys. Rev. E*, 96:032120, Sep 2017.
- [11] Y.-C. Lai and T. Tél. *Transient Chaos*. Springer, New York, 2011.
- [12] Andrey V. Polovinkin, Evgeniya V. Pankratova, Dmitriy G. Luchinsky, and Peter V. E. McClintock. Resonant activation in single and coupled stochastic FitzHugh-Nagumo elements. *Proc.SPIE*, 5467:5467–5467–10, 2004.
- [13] A. Hamm, T. Tél, and R. Graham. Noise-induced attractor explosions near tangent bifurcations. *Physics Letters A*, 185(3):313–320, 1994.
- [14] R. Graham, A. Hamm, and T. Tél. Nonequilibrium potentials for dynamical systems with fractal attractors or repellers. *Phys. Rev. Lett.*, 66:3089–3092, Jun 1991.
- [15] M. Evans, N. Hastings, and B. Peacock. *Statistical Distributions*. Wiley, New York, 2000.
- [16] M. Abramowitz and I. A. Stegun. *Handbook of Mathematical Functions with Formulas, Graphs, and Mathematical Tables*. Dover, New York, 1972.
- [17] S. Coles. *An Introduction to Statistical Modeling of Extreme Values*. Springer, 2001.
- [18] P. E. Kloeden and E. Platen. *Numerical Solution of Stochastic Differential Equations*. Springer, 1995.
- [19] Paul F. Hoffman and Daniel P. Schrag. The snowball Earth hypothesis: testing the limits of global change. *Terra Nova*, 14(3):129–155, 2002.
- [20] M. Ghil. Climate stability for a Sellers-type model. *J. Atmos. Sci.*, 33:3–20, 1976.
- [21] Tamás Bódai, Valerio Lucarini, Frank Lunkeit, and Robert Boschi. Global instability in the ghil-sellers model. *Climate Dynamics*, 44(11):3361–3381, 2014.
- [22] <https://uk.mathworks.com/matlabcentral/fileexchange>
- [23] William H. Press, Saul A. Teukolsky, William T. Vetterling, and Brian P. Flannery. *Numerical Recipes 3rd Edition: The Art of Scientific Computing*. Cambridge University Press, New York, NY, USA, 3 edition, 2007.